STATIC DROP FORMATION IN AN ELECTROSTATIC FIELD

TAKAO TSUKADA, MASAKAZU SATO, NOBUYUKI IMAISHI,
MITSUNORI HOZAWA AND KATSUHIKO FUJINAWA
Chemical Research Institute of Non-Aqueous Solutions,
Tohoku University, Sendai 980

Key Words: Drop Formation, Electrostatic Field, Drop Shape, Numerical Simulation, Boundary Element Method, Finite Element Method

Drop formation in uniform and non-uniform electric fields was studied theoretically and experimentally. In the analyses, the electric field and the drop shape were calculated numerically by use of the boundary element method and the finite element method, respectively.

It is found that the experimental maximum drop volume in a uniform electric field can be predicted well by analysis and that the experimental drop profile and the drop charge are in agreement with the calculated ones.

The theoretical values of the maximum drop volume in a non-uniform electric field are found to agree with the experimental results of previous workers.

Introduction

As it is of great importance to know the mechanism of drop formation in an electrostatic field for the design of electrostatic spray painting devices, high speed printers and electrostatic liquid-liquid extraction apparatus, many experimental works[3-6] have been carried out.

Watanabe[6] studied electrostatic drop formation from a metal capillary in the air and found that the drop shape depends on the electrical conductivity of the drop.

Takamatsu *et al.*[3-5] investigated drop formation in uniform and non-uniform electric fields for liquid-gas and liquid-liquid systems and analyzed the drop volume and the drop charge theoretically under the assumption of a spherical drop.

Recently, Adornato *et al.*[1] calculated the shape and the stability of an electrostatically levitated drop by use of the finite element method.

For drop formation in a uniform or non-uniform electric field, however, there have been no reports which determine the electrostatic field and the drop shape simultaneously.

The aim of this work is to analyze theoretically the electrostatic field and the drop shape by use of the boundary element method[7] and the finite element method[1,2] respectively, and to confirm experimentally the validity of the theoretical analyses.

1. Theory

Drop formation in uniform and non-uniform electric fields is considered here.

Figure 1(a) shows the cylindrical coordinates for the uniform electric field, where the upper plate is the anode and the lower one is the cathode. For the non-uniform field, one of the parallel plate electrodes is replaced by a vertical nozzle as shown in **Fig. 1(b)**. It is assumed that the liquid drop is a conductor and the surface potential is the same as that of the anode, and that the ambient fluid is an insulator.

The governing equation for the electric field is given by the following Laplace equation,

$$\nabla'^2\phi'=0 \tag{1}$$

The boundary conditions for the uniform electric field are expressed by Eq. (2),

at anode plane ($R'_a \leqq r' \leqq r'_w$, $z'=0$):

$$\phi'=\phi'_0 \tag{2-1}$$

at cathode plane ($0 \leqq r' \leqq r'_w$, $z'=h'$):

$$\phi'=0 \tag{2-2}$$

at side wall ($r'=r'_w$, $0 \leqq z' \leqq h'$):

$$\partial\phi'/\partial n'=0 \tag{2-3}$$

at drop surface:

$$\phi'=\phi'_0\,. \tag{2-4}$$

For the non-uniform electric field, the boundary conditions are given by Eq. (3),

at nozzle surface ($r'=R'_a$, $z'_w \leqq z' \leqq 0$):

$$\phi'=\phi'_0 \tag{3-1}$$

at cathode plane ($0 \leqq r' \leqq r'_w$, $z'=h'$):

$$\phi'=0 \tag{3-2}$$

Received March 24, 1986. Correspondence concerning this article should be addressed to T. Tsukada. M. Sato is now with Shin-Etsu Handotai Co., Ltd., Fukushima 961.

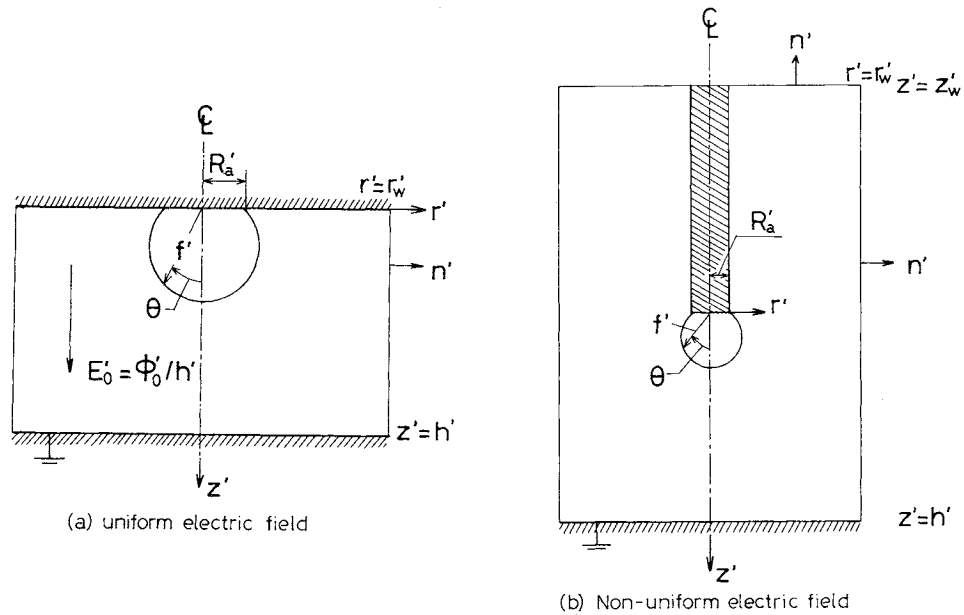

Fig. 1. Cylindrical coordinates.

at upper wall ($R_a' \leqq r' \leqq r_w'$, $z'=z_w'$):

$$\partial\phi'/\partial n'=0 \tag{3-3}$$

at side wall ($r'=r_w'$, $z_w' \leqq z' \leqq h'$):

$$\partial\phi'/\partial n'=0 \tag{3-4}$$

at drop surface:

$$\phi'=\phi_0' \tag{3-5}$$

where ϕ' and $\partial\phi'/\partial n'$ are the electric potential and its normal derivative respectively. Accordingly, the electric field around the drop is given by solving Eq. (1) under the boundary conditions.

As the outward electrostatic force acts on the drop surface in the electric field, the drop is more elongated than that in the absence of the field. The drop shape can be obtained by solving the modified Young-Laplace equation[1] as follows.

$$2H'\sigma=\Delta p'+\varepsilon_0(\partial\phi'/\partial n')^2/2 \tag{4}$$

where the second term of the right-hand side corresponds to the electrostatic stress.

The drop volume is given by Eq. (5), using the spherical coordinates shown in Fig. 1.

$$V'=(2/3)\pi\int_0^{\pi/2} f'^3\sin\theta d\theta \tag{5}$$

The boundary conditions are expressed as follows.

$$\partial f'/\partial\theta=0 \quad \text{at} \quad \theta=0 \tag{6-1}$$

$$f'=R_a' \quad \text{at} \quad \theta=\pi/2 \tag{6-2}$$

To obtain the electric field from Eqs. (1) and (2) or (3), the boundary element method (B.E.M.)[7] was used. For the drop shape, the Galerkin finite element method (F.E.M.)[1] was applied to Eqs. (4)–(6). **Figure 2** shows the discretization of the calculation domain. The boundary element formulations and the finite element formulations in dimensionless expressions are described in **Appendices 1** and **2**, respectively.

The numerical calculations were carried out by use of ACOS 1000 of the Computer Center of Tohoku University.

2. Experimental Apparatus and Procedure

Figure 3 shows the experimental apparatus, which is almost the same as that of Takamatsu *et al.*[3] Two brass parallel-plate electrodes (150 mm × 150 mm), the upper one of which was connected to a D.C. High Voltage (H.V.) generator and the other was grounded, were used. Distilled water was fed from a microfeeder to the nozzle set in the center of the upper electrode, and single drops were formed. The inertial effect was negligible because of the slow rate of drop formation; it was approximately 1 drop per 3 min. After D.C. high voltage (0–20 kV) was applied, the drop shape was photographed periodically. The drop volume was calculated from numerical integration of the profile. Nozzles of 1–5 mm O.D. were used and the distance between the electrodes was 2.9 cm or 4 cm.

The charge of a drop falling through a hole in the lower electrode was measured by an electrometer connected to a Faraday cage.

The whole experimental system was set in an air bath of 298 K.

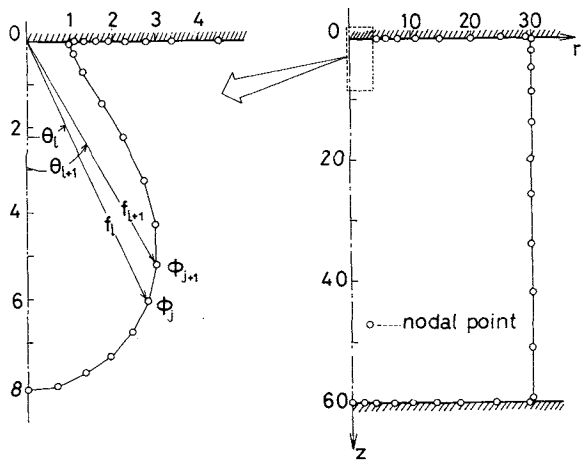

Fig. 2. Discretization of calculation domain.

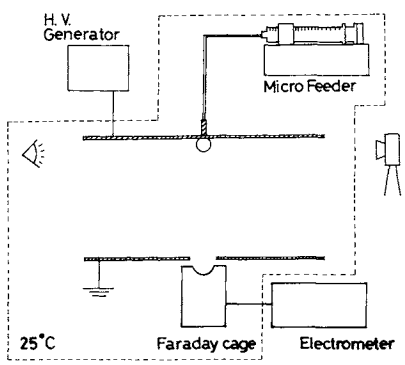

Fig. 3. Experimental apparatus.

3. Results and Discussion

3.1 Drop shape and maximum drop volume in uniform electric field

Figure 4 shows the effect of electric fields on the drop shape for $Bo=-0.543$. The profiles on the left-hand side show the calculated drop shapes[2] of various volume at $E_0'=0$ and those on the right-hand side are those at $E_0'=3.53\times10^5$ V/m. The plotted circles show the experimental results. Apparently, the drop profiles in the electric field are elongated downward by the electrostatic force, in comparison with those in the absence of the electric field. The calculated profiles are found to agree well with the experimental ones.

Figure 5 gives the contour lines of dimensionless electric potential for $V=1.053$ in Fig. 4(b), where the interval of the contour lines around the drop is five times as fine as that in the other region.

To obtain the maximum stable drop volume, a stability analysis was carried out. According to the bifurcation analysis[1] of interface stability, the shape stability changes only through the neutrally stable state for a parameter value. This state corresponds to either the bifurcation point to new shape families, or the limit point at which no equilibrium shape exists for parameter values larger than the critical value.

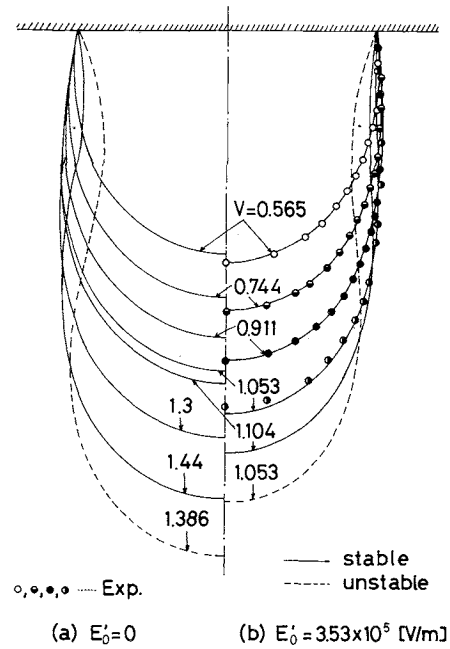

Fig. 4. Effect of electric field on drop shape ($Bo=-0.543$).

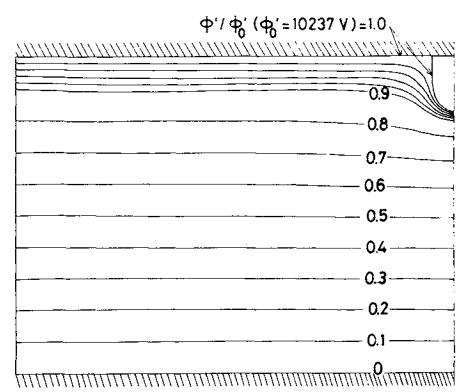

Fig. 5. Contour lines of electric potential for $Bo=-0.543$, $E_0'=3.53\times10^5$ V/m and $V=1.053$.

The system considered here has only the limit point and this value is obtained by rewriting the equation set for a new parameter in terms of which the family of drop shape is single-valued, at least near the limit point. In this work reference pressure difference κ is used as a new parameter, instead of dimensionless drop volume V.

Figure 6 shows the stability analysis of the equilibrium shape. In each electric field strength E_0', V takes the maximum value at the limit point. The broken lines show the region of the unstable equilibrium shape and no real shapes in this region exist. The profiles shown by the broken lines in Fig. 4 correspond to the unstable equilibrium drop shapes.

In **Fig. 7**, the experimental relations between the maximum drop volume V'_{max} and E_0' for various nozzle radii R_a' are given. Apparently, V'_{max} becomes smaller as E_0' becomes larger. The experimental values are in good agreement with the theoretical pre-

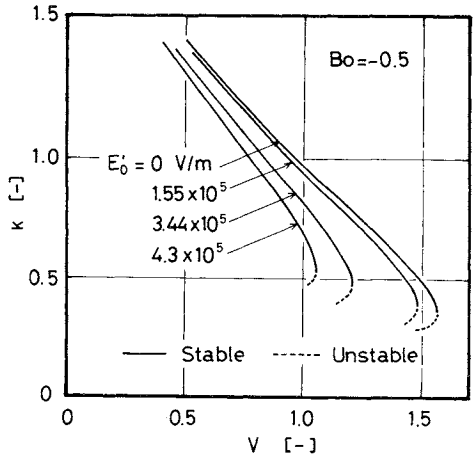

Fig. 6. Stability analysis of equilibrium drop shapes.

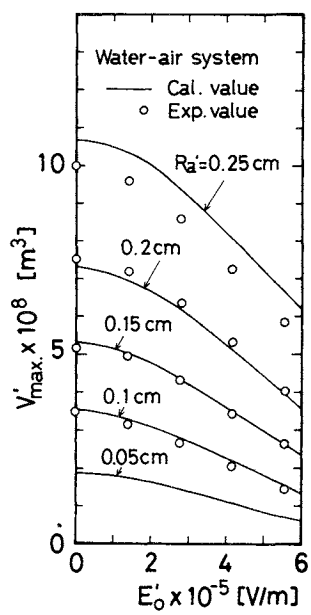

Fig. 7. Effect of E'_0 on V'_{max}.

dictions based on the stability analysis.

Figure 8 shows the experimental relations between the residual drop volume V'_{min} which remains on the nozzle after the fall of the drop, and E'_0. V'_{min} increases with E'_0, but decreases rapidly beyond some E'_0, $E'_{0,crit}$, and approaches zero. $E'_{0,crit}$ becomes smaller as the nozzle radius R'_a becomes larger. It was observed experimentally that the drop formed a long liquid jet at the instant of falling when E'_0 was larger than $E'_{0,crit.}$.

3.2 Drop surface charge

Figure 9 shows the effect of the electric field strength on the drop surface charge Q' for $R'_a=0.5$ mm in the uniform electric field. Q' is calculated from the following equation.

$$Q' = -\varepsilon_0 \int_{S'} (\partial\phi'/\partial n')dS' \qquad (7)$$

It is seen from the theoretical result that Q' takes a

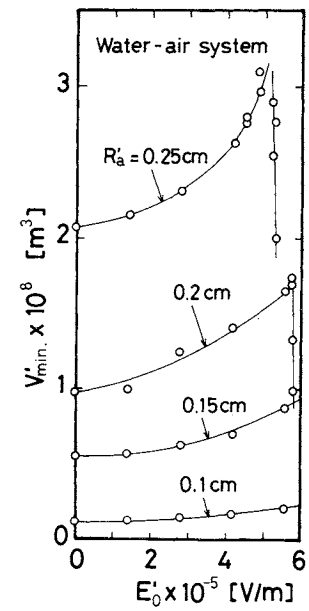

Fig. 8. Experimental relations between V'_{min} and E'_0.

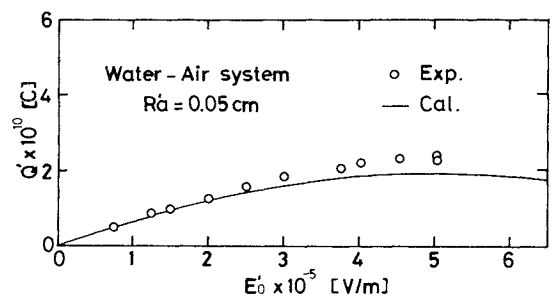

Fig. 9. Effect of E'_0 on drop surface charge Q'

maximum value at some E'_0. The maximum value was observed by Takamatsu *et al.*[3] experimentally. This is due to the reduction of the surface area because the maximum drop volume becomes smaller as E'_0 increases. The theoretical results agree with our experimental results.

3.3 Drop formation in non-uniform electric field

Figure 10 shows the calculated relations between the applied voltage ϕ'_0 and the maximum drop volume V'_{max} for drop formation in a non-uniform electric field, where one electrode is a vertical nozzle with 2.6 mm O.D. and the other is a flat plate, as shown in Fig. 1(b), and the distance between them is 5 cm. The dotted line shows the calculated result in the uniform electric field where the distance between the electrodes is 5 cm. The plots show the experimental results of Takamatsu *et al.*[5] and are in good agreement with the theoretical prediction. Apparently, V'_{max} is considerably small in comparison with the case in the uniform electric field for the same applied voltage. This is due to the larger electric field strength on the drop surface, for the contour lines of the electric potential around the drop are dense, as shown in **Fig. 11**.

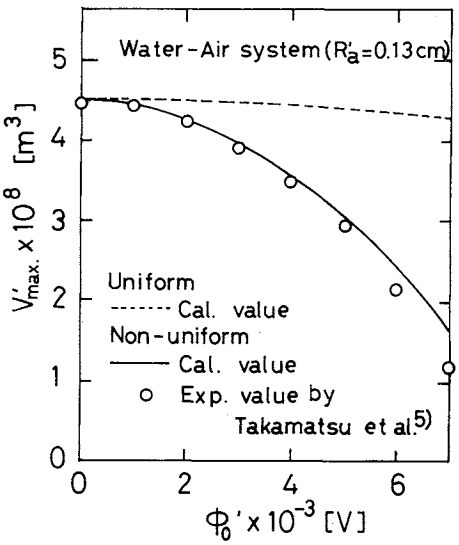

Fig. 10. Effect of applied voltage on V'_{max} in non-uniform electric field.

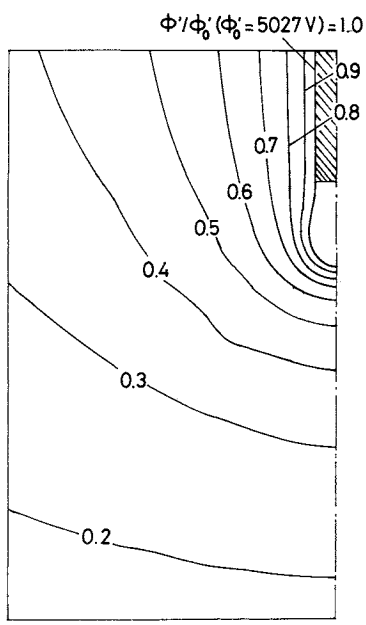

Fig. 11. Contour lines of electric potential around drop for $V' = 3.06 \times 10^{-8}$ m^3 in non-uniform electric field.

Conclusion

Drop formation in the electric field was studied experimentally and theoretically and the following conclusions were obtained.

The maximum drop volume in uniform and non-uniform electric fields decreases as the electric potential increases and can be predicted by a stability analysis of the equilibrium drop shape.

The drop profiles and the charge of the drop surface agree well with the calculations.

Appendix 1

To obtain the electric field, Eq. (1) is solved by use of the boundary element method.[7] Firstly, the weighted residual statement of Eq. (1) is integrated twice by part, in which the weighted function, namely the fundamental function ϕ^*, must satisfy the governing equation:

$$\nabla^2\phi^* + \delta_i = 0 \tag{A-1}$$

where δ_i is the Dirac delta function. "i" is the source point representing the singularity in the delta function and is set on the boundary surface S of the domain to formulate the boundary problem.

The boundary integral equation with ϕ^* is expressed as follows.

$$c_i\phi_i + \int_S \phi(\partial\phi^*/\partial n)dS = \int_S (\partial\phi/\partial n)\phi^* dS \tag{A-2}$$

where ϕ and $\partial\phi/\partial n$ are electric potential and its normal derivative, c_i is the unknown coefficient, ϕ_i is potential in "i", and ϕ^* and $\partial\phi^*/\partial n$ are given as follows.

$$\phi^* = 1/4\pi R \tag{A-3}$$

$$\partial\phi^*/\partial n = -(1/4\pi R^2)(\partial R/\partial n) \tag{A-4}$$

in which R is the distance between the source "i" and the appropriate point.

To solve the above equations, the boundary surface S is discretized with the finite elements, as shown in Fig. 2, and the potential and its normal derivative in each element are approximated by Eqs. (A-5) and (A-6).

$$\phi = \sum\psi_j\phi_j \tag{A-5}$$

$$\partial\phi/\partial n = \sum\psi_j(\partial\phi/\partial n)_j \tag{A-6}$$

where ψ_j is the linear trial function. Substituting Eqs. (A-5) and (A-6) into the above equations, the set of algebraic equations is obtained. The potential and its normal derivative are given by solving the equations.

Appendix 2

To solve Eq. (4) with Eqs. (5) and (6), the Galerkin finite element method is used. In each finite element in Fig. 2, dimensionless radial distance in spherical coordinates is approximated as follows, where the characteristic length is the radius of nozzle R'_a.

$$f = \sum\chi_l f_l \tag{A-7}$$

χ_l is the Hermite cubic trial function.

Substitution of Eq. (A-7) into the dimensionless form of Eq. (4) gives the algebraic equations as follows.

$$\int_S \chi_l\{2H + Bo\cdot f\cdot\cos\theta - \kappa - (\partial\phi/\partial n)^2/8\pi\}dS = 0 \tag{A-8}$$

where Bo is the Bond number. To solve Eq. (A-8) for the drop shape, the Newton-Raphson iterative method is used.

Nomenclature

Bo	=	Bond number ($=(\rho_0-\rho)R_a'^2 g/\sigma$)	[—]
c_i	=	unknown coefficient	[—]
E'_0	=	electric field strength	[V·m^{-1}]
$E'_{0,crit.}$	=	critical electric field strength	[V·m^{-1}]
f'	=	radial distance in spherical coordinates	[m]
f	=	f'/R'_a	[—]
g	=	gravitational acceleration	[m·s^{-2}]
H'	=	mean curvature	[m^{-1}]
H	=	$H'R'_a$	[—]
h'	=	distance between electrodes	[m]
n'	=	normal distance from surface	[m]

n	=	n'/R'_a	[—]
$\Delta p'$	=	pressure difference across drop surface	[Pa]
Q'	=	drop surface charge	[C]
R	=	distance between source and observation points	[—]
R'_a	=	radius of nozzle	[m]
r'	=	radial distance in cylindrical coordinates	[m]
r	=	r'/R'_a	[—]
r'_w	=	distance between center line and side wall	[m]
S'	=	boundary area	[m^2]
S	=	$S'/2\pi R'^2_a$	[—]
V'	=	drop volume	[m^3]
V	=	$V'/2\pi R'^3_a$	[—]
V'_{max}	=	maximum drop volume	[m^3]
V'_{min}	=	residual drop volume	[m^3]
z'	=	axial distance in cylindrical coordinates	[m]
z	=	z'/R'_a	[—]
z'_w	=	distance between nozzle tip and upper wall	[m]
ε_0	=	permittivity in vacuum	[$F \cdot m^{-1}$]
θ	=	polar angle in spherical coordinates	[rad]
κ	=	reference pressure difference ($=\Delta p' R'_a/\sigma$)	[—]
ρ	=	density of drop	[$kg \cdot m^{-3}$]
ρ_0	=	density of surrounding fluid	[$kg \cdot m^{-3}$]
σ	=	surface tension	[$mN \cdot m^{-1}$]
ϕ'	=	electric potential	[V]
ϕ'_0	=	electric potential on electrode and drop surface	[V]
ϕ	=	$\phi'(4\pi\varepsilon_0/\sigma R'_a)^{1/2}$	[—]
ϕ^*	=	fundamental solution	[—]
χ_i, ψ_i	=	trial function	[—]

Literature Cited

1) Adornato, P. M. and R. A. Brown: *Proc. R. Soc. London, Ser. A*, **389**, 101 (1983).
2) Hozawa, M., T. Tsukada, N. Imaishi and K. Fujinawa: *J. Chem. Eng. Japan*, **14**, 358 (1981).
3) Takamatsu, T., Y. Hashimoto, M. Yamaguchi and T. Katayama: *J. Chem. Eng. Japan*, **14**, 178 (1981).
4) Takamatsu, T., M. Yamaguchi and T. Katayama: *J. Chem. Eng. Japan*, **15**, 349 (1982).
5) Takamatsu, T., M. Yamaguchi and T. Katayama: *J. Chem. Eng. Japan*, **16**, 267 (1983).
6) Watanabe, A.: *Oyo Butsuri*, **37**, 314 (1968).
7) Yoshikawa, F. and M. Tanaka: *Transactions of JSME, Ser. B*, **50**, 1310 (1984).

AN ON-LINE OPERATING CONTROL SYSTEM FOR A CLASS OF COMBINED BATCH/SEMI-CONTINUOUS PROCESSES

KATSUAKI ONOGI, YOSHIYUKI NISHIMURA, YOSHIHIKO NAKATA AND TOSHIMITSU INOMATA

Department of Production Systems Engineering, Toyohashi University of Technology, Toyohashi 440

Key Words: Process System, Process Control, Systems Engineering, Batch Process, Semicontinuous Process, Operating Control System, On Line Control, Scheduling, Simulator, State Prediction

An operating control system for a class of combined batch/semi-continuous processes based on on-line scheduling is proposed. The class of controlled plants is characterized by a series of units with limited intermediate storage and statistical variabilities in processing time. The proposed system consists of a dynamical plant simulator and an automatic scheduler. The simulator predicts the future state of the plant using the past plant record, the present internal state of the plant and the temporal operating conditions. To make operation of the plant efficient and smooth, the scheduler revises the operating conditions on the basis of the predicted state. A series of simulation experiments has shown that the system is effective in plant operation with uncertainties.

Introduction

The increasing variety of variants in products and/or raw materials has enhanced the reconsideration of batch units because of their inherent flexibility. On the other hand, continuous units have advantages over batch units in systematic design procedure and stability of operation. Therefore, the introduction of combined batch/continuous processes into the process industry is becoming of great interest. However, there are very few studies on the operation of these combined processes.[3,4]

In actual operation of the plant, uncertainties usually occur which affect the performance of the whole plant. Operation of the plant which ignores these uncertainties may cause unexpected results, as

Received March 27, 1986. Correspondence concerning this article should be addressed to K. Onogi.